N-Hydroxyindole-based inhibitors of lactate dehydrogenase against cancer cell proliferation

ARTICLE *in* EUROPEAN JOURNAL OF MEDICINAL CHEMISTRY · SEPTEMBER 2011

Impact Factor: 3.45 · DOI: 10.1016/j.ejmech.2011.08.046 · Source: PubMed

European Journal of Medicinal Chemistry 46 (2011) 5398–5407

Contents lists available at SciVerse ScienceDirect

European Journal of Medicinal Chemistry

journal homepage: http://www.elsevier.com/locate/ejmech

Original article

N-Hydroxyindole-based inhibitors of lactate dehydrogenase against cancer cell proliferation

Carlotta Granchi[a], Sarabindu Roy[a], Alessio De Simone[a], Irene Salvetti[a], Tiziano Tuccinardi[a], Adriano Martinelli[a], Marco Macchia[a], Mario Lanza[b], Laura Betti[b], Gino Giannaccini[b], Antonio Lucacchini[b], Elisa Giovannetti[c], Rocco Sciarrillo[c], Godefridus J. Peters[c], Filippo Minutolo[a,*]

[a] *Dipartimento di Scienze Farmaceutiche, Università di Pisa, Via Bonanno 6, 56126 Pisa, Italy*
[b] *Dipartimento di Psichiatria, Neurobiologia, Farmacologia e Biotecnologie, Università di Pisa, Via Bonanno 6, 56126 Pisa, Italy*
[c] *Department of Medical Oncology, VU University Medical Center, De Boelelaan 1117, 1081 HV Amsterdam, The Netherlands*

ARTICLE INFO

Article history:
Received 22 July 2011
Received in revised form
29 August 2011
Accepted 31 August 2011
Available online 7 September 2011

Keywords:
Lactate dehydrogenase
Glycolysis
Warburg effect
Cancer
Hypoxia
Enzyme inhibitors

ABSTRACT

Current cancer research is being increasingly focused on the study of distinctive characters of tumour metabolism, resulting in a switch from oxidative phosphorylation to glycolysis (Warburg effect). Isoform 5 of human lactate dehydrogenase (*h*LDH5), which catalyzes the final step in the glycolytic cascade (pyruvate to lactate), constitutes a relatively new and untapped anti-cancer target. In this study, careful design and synthesis of a selected series of aryl-substituted *N*-hydroxyindole-2-carboxylates (NHIs) has led to several *h*LDH5-inhibitors, showing "first-in-class" potency and isoform selectivity. Enzyme kinetics studies indicated that these inhibitors exhibit a competitive mode of inhibition. Some representative examples were tested against two human pancreatic carcinoma cell lines, and displayed a good anti-proliferative activity, which was even more evident under hypoxic conditions.

1. Introduction

Neoplastic proliferation in hypoxia is characterized by an altered metabolism, which involves several crucial hallmarks of cancer, including a peculiar sugar metabolism [1]. Cell growth requires glucose as the most important source of energy, to generate adenosine-5′-triphosphate (ATP) molecules. Consequently, glucose consumption is generally increased in rapidly dividing cells, such as those constituting invasive tumour tissues. Furthermore, cancer cells are often exposed to hypoxic conditions, since oxygenation of tumours by vascularisation is usually less efficient. A metabolic switch from normal oxidative phosphorylation (OXPHOS) to anaerobic glycolysis, also known as the Warburg Effect [2], is very often found in invasive tumours. This adaptation allows malignant cells to produce ATP from glucose even in the absence of oxygen, by promoting the glycolytic process leading to the production of lactic acid. Therefore, the "glycolytic phenotype" confers cancer cells with an adaptation to otherwise hostile hypoxic environments, although the efficiency of this metabolic pathway is much lower when compared to that of OXPHOS [3]. For that reason, cancer cells exhibit an exaggerated avidity of glucose, as shown by the increased uptake of labelled glucose analogue ^{18}F-fluorodeoxyglucose (FDG), which is used to visualize *in vivo* invasive tumours [4]. Hence, this unique metabolic feature of invasive and hypoxic tumours, that does not occur in healthy tissues, is currently being considered as an ideal target for cancer-selective therapy [5].

There are several key-steps of the glycolytic process which are promoted by enzymes or transporters that have already been considered as suitable targets for an "anti-glycolytic" cancer therapy (Fig. 1).

Abbreviations: LDH, lactate dehydrogenase; NHI, *N*-hydroxyindole-2-carboxylate; ATP, adenosine-5′-triphosphate; OXPHOS, oxidative phosphorylation; FDG, ^{18}F-flurordeoxyglucose; GLUT-1, glucose membrane transporter; HK, hexokinase; GPI, glucose-6-phosphate isomerase; PFK, phospho-fructokinase; ALDO, aldolase; TPI, triosephosphate isomerase; GAPDH, glyceraldehyde-3-phosphate dehydrogenase; PGK, phosphoglycerate kinase; PGM, phosphoglycerate mutase; ENO, enolase; PK, pyruvate kinase; PDK, dehydrogenase kinase; DCA, dichloroacetate; PDH, pyruvate dehydrogenase; IDH, isocitrate dehydrogenase; NADH/NAD$^+$, nicotinamide adenine dinucleotide cofactor; TBAB, tetrabutylammonium bromide; DMF, *N,N*-dimethylformamide; MD, molecular dynamics; rmsd, root-mean-square deviation; DMSO, dimethylsulfoxide; HPLC, high performance liquid chromatography; TLC, thin-layer chromatography; NMR, nuclear magnetic resonance; EI, electron impact; MS, mass spectroscopy; t_R, retention time; RT, room temperature; CG, conjugated gradient.

* Corresponding author. Tel.: +39 050 2219557; fax: +39 050 2219605.
E-mail address: filippo.minutolo@farm.unipi.it (F. Minutolo).

0223-5234/$ – see front matter © 2011 Elsevier Masson SAS. All rights reserved.
doi:10.1016/j.ejmech.2011.08.046

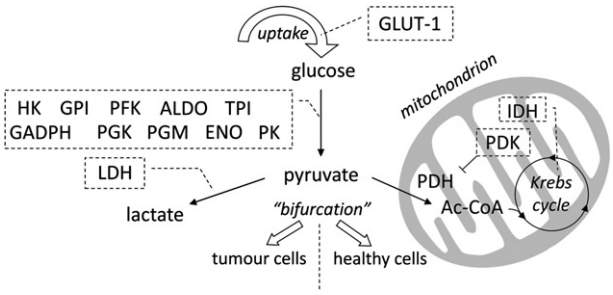

Fig. 1. Targets of glucose metabolism considered for anti-cancer treatment.

Some enzymes/transporters promoting the degradation of glucose to pyruvate have been targeted by perspective anti-cancer agents: glucose membrane transporter (GLUT-1), hexokinase (HK), glucose-6-phosphate isomerase (GPI), phospho-fructokinase (PFK), aldolase (ALDO), triosephosphate isomerase (TPI), glyceraldehyde-3-phosphate dehydrogenase (GAPDH), phosphoglycerate kinase (PGK), phosphoglycerate mutase (PGM), enolase (ENO), pyruvate kinase (PK) [5d]. However, inhibitors of these factors are also expected to interfere with the metabolism of normal cells, because they are placed before the "bifurcation" point of pyruvate, whose destiny depends on the cellular context (tumour *vs.* healthy cells), as well as on the amount of oxygen available. An interesting exception is represented by selective inhibitors of isoform M2 of PK, which is only found in foetal and cancer cells [6]. Nevertheless, the real role of PK-M2 in either tumour suppression or carcinogenesis is currently being debated, because paradoxical effects were reported as associated to PK-M2 inhibition/activation, so it is still not clear if and when it promotes or suppresses tumours [7]. Enzymes operating inside mitochondria were also considered as suitable targets for cancer chemotherapy. One of them is pyruvate dehydrogenase kinase (PDK), whose inhibition by dichloroacetate (DCA) restores the activity of pyruvate dehydrogenase (PDH) and re-activates OXPHOS in cancer cells, thus leading them to apoptosis [8]. Another attractive target in this context is isocitrate dehydrogenase (IDH), whose mutated form present in several tumours is currently being considered for therapeutic opportunities [9]. Within this picture, we focused our attention on lactate dehydrogenase (LDH). In fact, the metabolic position of this enzyme, right after the "bifurcation" of the pyruvate destinies, would be ideal for a selective intervention against cancer, since its inhibition would only involve cells where OXPHOS is mostly compromised, such as tumour cells. This means that a block of the glucose metabolism at this stage should not be expected to present relevant toxic effects to most normal cells, which exploit the normal mitochondrial degradation of pyruvate.

LDH is an oxidoreductase which catalyzes the interconversion of pyruvate and lactate by using a nicotinamide adenine dinucleotide cofactor ($NADH/NAD^+$). Human LDH is a tetrameric enzyme which may be composed by three different monomeric subunits: LDH-A, LDH-B and LDH-C. While the C subunit takes only part of a homotetrameric enzyme, *h*LDHX (LDH-C_4), which plays a role in male fertility [10], the A and B subunits are found to be combined in five tetrameric isoforms (*h*LDH1-5) constituted of homotetramers, such as *h*LDH1 (LDH-B_4) and *h*LDH5 (LDH-A_4), and heterotetramers made of the other three possible combinations of A and B subunits (*h*LDH2-4) [11]. Localization of *h*LDH1 is mostly limited to the heart, where it generally catalyzes the oxidation of lactate to pyruvate, whereas isoform *h*LDH5 preferentially catalyzes the reduction of pyruvate to lactate and is the main form present in skeletal muscles and liver [12]. Overexpression of isoform 5 was detected in highly invasive and hypoxic carcinomas [13]. and oxygen deprivation induced gene expression of LDH-A subunit in cancer cell cultures media [14]. A validation of *h*LDH5 as an anti-cancer target derived from studies conducted on LDH-A-deprived cancer cell lines, which demonstrated that gene repression of the production of the LDH-A subunit in cancer cells by shRNA seriously compromised the tumour growth and invasiveness of these LDH-A-deficient cells under hypoxia [15]. In addition, studies on naturally occurring knock-out human "models", constituted by individuals affected by hereditary LDH-A deficiency, show that the lack of this enzyme does not cause any symptoms under ordinary circumstances, whereas muscle damage and myoglobinuria are observed only after intense anaerobic exercise [16]. These evidences would further confirm the high possibility for *h*LDH5 to be a safe target for anti-tumour agents.

Not until very recent times do we find examples of efficient LDH-inhibitors, because only very few clinical applications were so far envisioned [17]. For example, reference LDH-inhibitor oxamic acid proved to reduce cellular growth in human hepatocellular carcinoma cell lines [18]. Furthermore, one of the very few efficient *h*LDH5-inhibitors reported in the literature, such as FX-11 (**1**, Fig. 2), was initially designed as an antimalarial agent [19]. FX-11 is a 2,3-dihydroxynaphtalen-1-carboxylate derivative, displaying a K_i value of 8 μM in the inhibition of *h*LDH5 and a >10-fold selectivity over the *h*LDH1 isoform, which proved to inhibit tumour progression by inducing an oxidative stress to the cancer cells [20]. Furthermore, a "bifunctional" butyric acid derivative (**2**, Fig. 2) was reported to inhibit *h*LDH5 with an IC_{50} value of 14.8 μM [21], although no data relative to cancer cell proliferation assays were reported.

Recently, we developed a new class of *N*-hydroxyindole-2-carboxylates (NHIs) [22], and those containing a phenyl ring at either 5 or 6 position (**3**, Fig. 2) displayed efficient and isoform-selective inhibition of *h*LDH5, with K_i values reaching the low micromolar range [22a]. These compounds also proved to sensibly decrease cellular lactate production and caused a marked reduction of cancer cell proliferation, especially under hypoxic conditions [22a].

In the light of these results, we decided to further investigate and expand this series of 5/6-phenyl-substituted NHIs by introducing chemical variability at the aryl substituents of the NHI central core. Details of the parallel synthetic routes that were developed, along with analysis of the activity of the analogues generated on isolated *h*LDH5 and *h*LDH1 isoforms, and against cancer cells *in vitro* are reported.

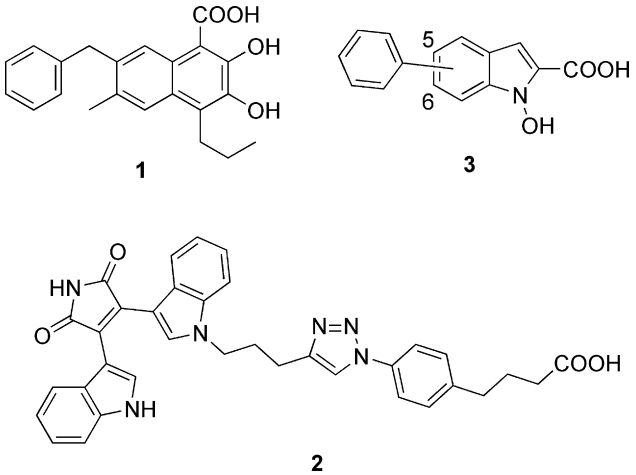

Fig. 2. Structures of *h*LDH5-inhibitors: FX-11 (**1**), a "bifunctional" butyric acid derivative (**2**), and 5/6-phenyl-substituted NHIs (**3**).

2. Chemistry

A series of 5- and 6-arylsubstituted NHIs (**3a**–**t**) were synthesized, by utilizing a general pathway which is displayed in Scheme 1. In each case, different conditions were chosen on the basis of preliminary optimizations of the reaction outcome, which proved to be highly dependent on the precursor structure. This synthesis started with the initial formation of aryl-substituted nitrotoluene intermediates **8a**–**t**, which were obtained by cross-coupling reactions performed under various conditions (*methods A* and *B*, Scheme 1). In details, 4-chloro-2-methyl-1-nitrobenzene (**4**) efficiently underwent Pd-catalyzed cross-coupling reactions with the appropriate arylboronic acid $R^1B(OH)_2$ under either classical Suzuki conditions [23], or phosphine-free conditions comprising the use of tetrabutylammonium bromide (TBAB) as the phase-transfer agent, in the presence of sodium carbonate upon microwave irradiation [24]. It should be noted that **4**, in spite of being an aryl chloride which is notoriously less reactive under the conditions reported in *methods A* and *B*, it possesses a nitro-group in *para*-position to the reactive chloro atom which activates this compound toward the cross-coupling reaction. This way, we were able to efficiently insert the R^1-substituent and produce intermediates **8a**–**e**.

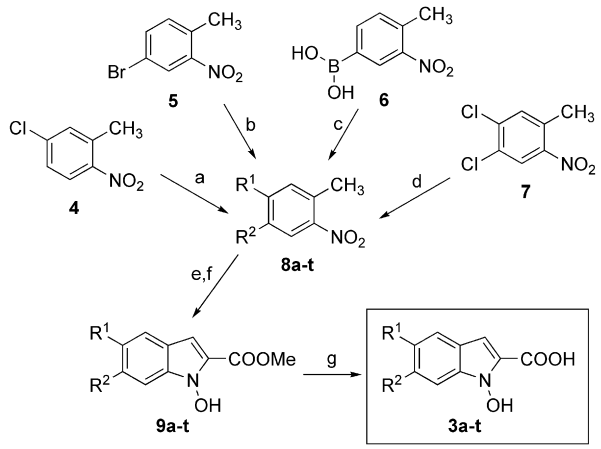

	R^1	R^2		R^1	R^2
a	4-Cl-Ph	H	**m**	H	4-(2-carboxyethyl)-Ph
b	4-F-Ph	H	**n**	H	4-CF_3O-Ph
c	4-CF_3-Ph	H	**o**	H	3-CF_3O-Ph
d	4-CH_3O-Ph	H	**p**	H	4-CH_3O-Ph
e	3-carboxy-Ph	H	**q**	H	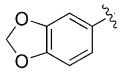
f	H	4-Cl-Ph			
g	H	2,4-Cl_2-Ph			
h	H	4-F-Ph	**r**	H	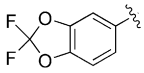
i	H	4-CF_3-Ph			
j	H	4-Ph-Ph			
k	H	α-naphthyl	**s**	H	3-furyl
l	H	β-naphthyl	**t**	Ph	Ph

Scheme 1. Synthesis of NHIs **3a**–**t**. Reagents and conditions: a) *method A*: $R^1B(OH)_2$, $Pd(OAc)_2$, PPh_3, aq 2M Na_2CO_3, toluene, EtOH, 100 °C, 24 h (**8a,e**); *method B*: $R^1B(OH)_2$, $Pd(OAc)_2$, TBAB, Na_2CO_3, H_2O, μW, 5 min (**8b**–**d**); b) *method A*: $R^2B(OH)_2$, $Pd(OAc)_2$, PPh_3, aq 2M Na_2CO_3, toluene, EtOH, 100 °C, 24 h (**8f,g,m**) or μW, 5 min (**8p**); *method B*: $R^2B(OH)_2$, $Pd(OAc)_2$, TBAB, Na_2CO_3, H_2O, μW, 20 min (**8j**–**l,n**), or K_3PO_4, H_2O 125 °C, 24 h (**8h,i**); c) R^2Br, $Pd(OAc)_2$, TBAB, Na_2CO_3, H_2O, μW, 5 min (**8o,q**–**s**); d) $PhB(OH)_2$, $Pd(OAc)_2$, TBAB, K_3PO_4, H_2O, 125 °C (sealed vial), 48 h (**8t**); e) $(COOMe)_2$, NaH, DMF, −15 °C to RT, 2–48 h; f) *method C*: $SnCl_2 \cdot 2H_2O$, anhydrous DME, 4 Å MS, 0 °C to RT, 6–16 h (**9d,p**); *method D*: 1) $SnCl_2 \cdot 2H_2O$, PhSH, Et_3N, CH_3CN, RT, 5 min, 2) *p*TsOH (cat.), toluene, evaporation under vacuum (**9a**–**c,f**–**l,n,o,q**–**s**); *method E*: $H_2PO_2Na \cdot 3H_2O$, Pd–C, H_2O/THF (1:1), RT; 24 h (**9e,m**); *method F*: Pb, TEAF, MeOH, 55 °C, 12 h (**9t**); g) aq 2 N LiOH, THF/MeOH (1:1), RT, 1–16 h.

The introduction of the R^2-substituent was obtained in two different ways: in some cases 4-bromo-1-methyl-2-nitrobenzene (**5**) was reacted with boronic acids $R^2B(OH)_2$, whereas in other cases we found it convenient to react 4-methyl-3-nitrophenylboronic acid (**6**) with the aryl bromides R^2-Br, as reported in details in the Experimental Section. In particular, compounds **8f**–**n** were obtained by reacting the appropriate $R^2B(OH)_2$ with bromo-aryl **5**. Most of these reactions were carried out under ligand-free conditions (*method B*), in the presence of either Na_2CO_3 upon microwave irradiation [24], to get compounds **8j**–**l,n**, or K_3PO_4 under conventional heating [25], to produce intermediates **8h,i**. Carboxy-substituted intermediate **8m** could only be obtained in the presence of a phosphine ligand, by generating *in situ* the $Pd(PPh_3)_4$ catalyst (*method A*). A particular care was necessary during the preparation of 4-chlorophenyl- and 2,4-dichlorophenyl-substituted intermediates **8f** and **8g**, respectively. In fact, when we employed microwave conditions to the preparation of these compounds, we obtained complex reaction mixtures, probably deriving from over-reactions of the chloro-aryl portions under those harsh conditions. Therefore, we had to switch back to classical thermal $Pd(PPh_3)_4$–catalyzed Suzuki conditions, so that, in spite of prolonged reaction times (24 h) required to get satisfactory conversions, **8f** and **8g** could be easily obtained and purified. Nitrotoluene derivatives **8o,q–s** were, instead, obtained starting from boronic acid **6**, which was reacted with the required aryl bromide R^2-Br. In this case, all the cross-coupling reactions could be efficiently carried out under the same ligand-free microwave-assisted conditions [24], to produce the required intermediates. Finally, the contemporary insertion of two phenyl ring in the structure of 1,2-dichloro-4-methyl-5-nitrobenzene (**7**) [26] was obtained under phosphine-free thermal cross coupling conditions in the presence of K_3PO_4 [25].

The subsequent sequence of reactions involved a base-promoted condensation of **8a–t** with dimethyloxalate, followed by a reductive cyclization, initiated by the partial reduction of the nitro- to hydroxylamine-group, to generate the *N*-hydroxyindole core (**9a**–**t**) [27]. While the first part of this sequence worked nicely under the same conditions for all the substrates, consisting in a deprotonation with sodium hydride in anhydrous DMF and condensation with $(COOMe)_2$, which led to the formation of a α-ketoester intermediate [27], the subsequent reductive-cyclization step required a careful optimization in each case and proved to be highly dependent on the substrate. In fact, the main problem we encountered in this step was the possible over-reduction of the nitro group, which led to the formation of variable amounts of N–H indole side products, which were often difficult to separate from their desired N-OH analogues. One of the most commonly used methods reported in the literature for this purpose (*method C*), involving stannous chloride as the reducing agent [27,28], proved to be efficacious only in a few examples of ours (**9d,p**), whereas in most cases we had to turn to the addition of additives, such as thiophenol and triethylamine in acetonitrile (*method D*) [29], which allowed us to efficiently obtain compounds **9a**–**c,f**–**l,n,o,q**–**s**. This procedure gave a very quick (5 min) full conversion of starting material, but it required an additional treatment with a catalytic amount of *para*-toluenesulfonic acid (*p*-TsOH) and several cycles of dissolution in toluene and evaporation under vacuum of the toluene/water azeotrope, in order to obtain an exhaustive consumption of hydrated precursors of *N*-hydroxyindole derivatives **9**. In some restricted cases, these conditions did not guarantee the selective partial reduction of the nitro-group. Fortunately, the replacement of the tin-based reducing agent with either sodium hypophosphite in the presence of palladium on charcoal (*method E*) [30], or lead with tetraethylammonium formate in refluxing methanol (*method F*) [31], efficiently produced compounds **9e,m** and **9t**, respectively.

Hydrolysis of methyl-ester precursors **9a**–**t**, with lithium hydroxide in a 1:1 mixture of tetrahydrofuran and methanol, afforded final products **3a**–**t**.

3. *h*LDH5 and *h*LDH1 inhibition assays

The inhibitory activities of compounds **3a**–**t** on the two purified human enzyme isoforms *h*LDH5 and *h*LDH1 were measured by standard enzyme kinetics experiments. We first verified in a preliminary screening the percent inhibition of *h*LDH5 relative to control at a compound concentration of 125 μM in the presence of 25 μM NADH. Enzyme activity was determined by measuring the absorbance decrease at 340 nm, due to the consumption of NADH. Only compounds displaying a >50% inhibition at that concentration were further evaluated for a full enzyme kinetics characterization, to verify their type of inhibition versus both NADH and pyruvate, together with their isoform selectivity (*h*LDH5 *vs.* *h*LDH1). Hence, we initially evaluated the apparent Michaelis–Menten constants (K_m) relative to the cofactor (NADH) and the substrate (pyruvate) for *h*LDH5, measured from Lineweaver–Burk plots. Afterwards, we measured the apparent K_m' values in the presence of the selected inhibitors (concentration range = 25–100 μM). From the values of K_m' so obtained for each compound showing >50% inhibition at 125 μM, K_i values were determined by double-reciprocal Lineweaver–Burk plots and their values are reported in Table 1.

The first general observation deriving from these studies was that all the analyzed compounds are unable to inhibit *h*LDH1, since % inhibition of this isoform in the presence of 125 μM solutions of these compounds is always below 3%, with the single exception constituted by biphenyl-derivative **3j**, displaying a 44% inhibition of *h*LDH1 at 125 μM. Isoform *h*LDH5 is instead sensitive to the inhibitory action operated by many of these derivatives, as described below. This preference for isoform-5 had already been observed with 4- and 5-phenyl-substituted NHIs [22a].

Among the 5-monoaryl-substituted NHIs, only two compounds display appreciable levels of *h*LDH5-inhibition. Compound **3a**, bearing a *para*-chlorophenyl group, shows an efficient inhibition, at least in competition with NADH (K_i = 16 μM), comparable to the activity of its previously reported non-chlorinated counterpart [22a], whereas its competitive inhibition *vs.* pyruvate is considerably weaker (K_i = 100 μM). A similar level of inhibition *vs.* NADH is associated to **3e**, containing a 5-(3-carboxyphenyl) substituent, although this compound competes more efficiently than **3a** with pyruvate (K_i = 27 μM). When the aryl ring in position 5 contains a 4-fluoro- (**3b**), 4-trifluoromethyl- (**3c**), or a 4-methoxy-group (**3d**), the inhibitory activity is lost.

In contrast, a generally better inhibition of *h*LDH5 is obtained with 6-monoaryl-substituted NHIs, especially under pyruvate-saturating conditions (competition *vs.* NADH). Among these derivatives, *para*-Cl-phenyl-substituted NHI **3f** shows a potent NADH-competitive inhibition with a K_i as low as 5.3 μM, together with a less efficient K_i of 56 μM *vs.* pyruvate. The insertion of a second chlorine atom, as in 2,4-dichlorophenyl-substituted derivative **3g**, still preserves a good inhibitory activity *vs.* NADH (K_i = 9.8 μM) and contemporarily improves the competitive inhibition against the substrate (K_i = 28 μM). A slightly lower potency is associated to 4-fluoro- and 4-trifluoromethyl-substituted compounds **3h,i**, whereas biphenyl-derivative **3j** turns out to be very effective, with K_i values of 4.5 μM (NADH) and 14 μM (pyruvate), although its isoform selectivity is spoiled by a certain inhibition of *h*LDH1, as mentioned above. Naphthyl-substituted compounds **3k,l** have very similar inhibitory properties, with α-naphthyl-substituted **3k** being slightly more potent. A loss of activity is observed with **3m**, bearing a carboxyethyl-substituents in the *para*-position of the aryl ring, whereas both 4- and 3-trifluoromethoxy-substituted NHIs **3n** and **3o**, respectively, show a very efficient inhibition, especially *vs.* NADH, with K_i values in the 7.6–8.5 μM range. Substitution with alkoxy-groups (**3p,q**) affords inactive inhibitors, in agreement to the 5-substituted series (see **3d**), whereas the introduction of a *gem*-difluorobenzodioxolane portion (**3r**) or of a 3-furyl group (**3s**) produces inhibition levels that are more pronounced *vs.* pyruvate (K_i = 17–20 μM) than *vs.* NADH (K_i = 52–54 μM). Finally, compound **3t**, containing phenyl rings in both positions 5 and 6, shows excellent levels of inhibition in both competition assays, with K_i values of 5.4 μM (vs. NADH) and 7.5 μM (vs. pyruvate).

The competitive behaviour of these inhibitors was demonstrated by the fact that different concentrations of each active compound does not change the V_{max} of the enzyme kinetics, but it only changes the K'_m value. This is also graphically displayed by the Lineweaver–Burk plot of a representative example constituted by compound **3g** (Fig. 3), where the competitive behaviour *vs.* both the cofactor (panel a) and the substrate (panel b) is demonstrated.

Table 1
*h*LDH5 inhibition data for selected NHI derivatives (**3**).

Entry	Compound	K_i [μM][a] (*vs.* NADH[b]	K_i [μM][a] (*vs.* Pyr)[c]
1	**3a**	16	100
2	**3e**	19	27
3	**3f**	5.3	56
4	**3g**	9.8	28
5	**3h**	67	17
6	**3i**	42	25
7	**3j**[d]	4.5	14
8	**3k**	10	7.1
9	**3l**	15	13
10	**3n**	7.6	40
11	**3o**	8.5	33
12	**3r**	52	17
13	**3s**	54	20
14	**3t**	5.4	7.5

[a] Values are reported as the average of three or more measurements; the error in these values is within ±30% of the average.
[b] Saturating concentration (2.0 mM) of sodium pyruvate and competitive increasing concentrations (12.5 ÷ 150 μM) of NADH.
[c] Saturating concentration (200 μM) of NADH and competitive increasing concentrations (25 μM ÷ 1.0 mM) of sodium pyruvate.
[d] This compound also showed a 44% inhibition of isoform *h*LDH1 at 125 μM.

4. Molecular modelling

In order to further characterize the interaction of these new compounds with the *h*LDH5 active site, one of the most potent inhibitors of this series (**3g**) was docked into the minimized average structure of LDH-A chain, which was recently obtained by us [22] and then subjected to 10 ns of molecular dynamics (MD) simulations. The analysis of the root-mean-square deviation (rmsd) from the initial model of the α carbons of the proteins showed that, after an initial increase, the rmsd remained approximately constant around 1.4 Å during the last 7 ns (Supplementary Data, Fig. S1). Fig. 4 shows the minimized structure of the average of the last 7 ns of the MD simulation. In agreement with our previously reported binding hypothesis [22], the carboxylic group of compound **3g** shows polar interactions with R169 and T248, and the *N*-hydroxy group displays an H-bond with the backbone nitrogen atom of T248, as well as with a water molecule that mediates the interaction with H193.

As shown in Table 2, the H-bond analysis of the MD simulation confirms the stability of these interactions, since during the last 7 ns all the indicated interactions are highly conserved during the MD simulation (49–99% occupied populations).

The indole central scaffold is placed in a cleft mainly delimited by N138, A238, V241, T248, I252 whereas the aryl group is inserted

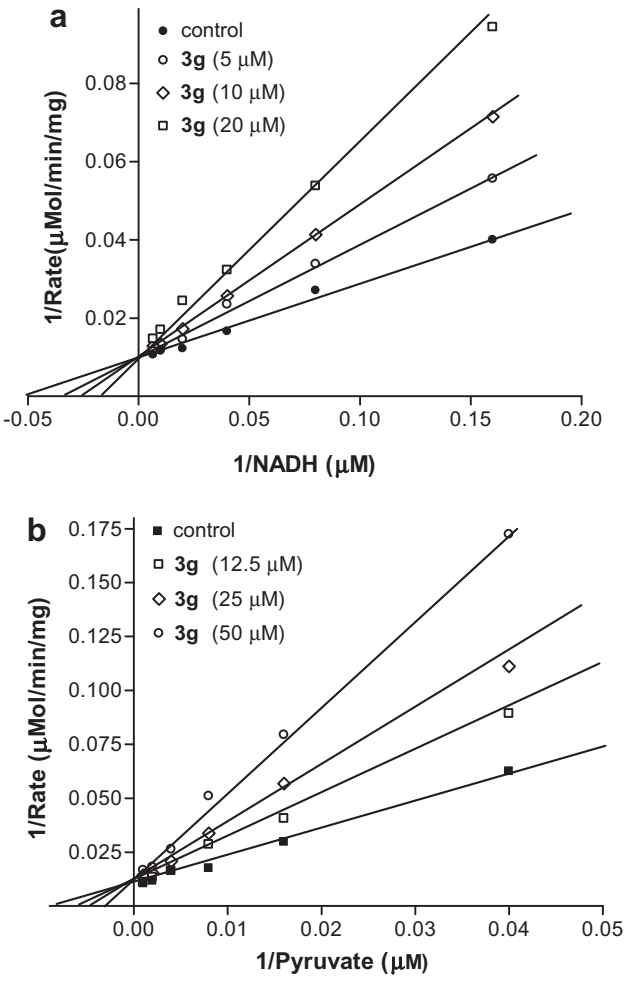

Fig. 3. Lineweaver–Burk plots showing the mode of inhibition of a representative NHI (**3g**). Linear competitive inhibition with respect to: a) NADH; b) pyruvate.

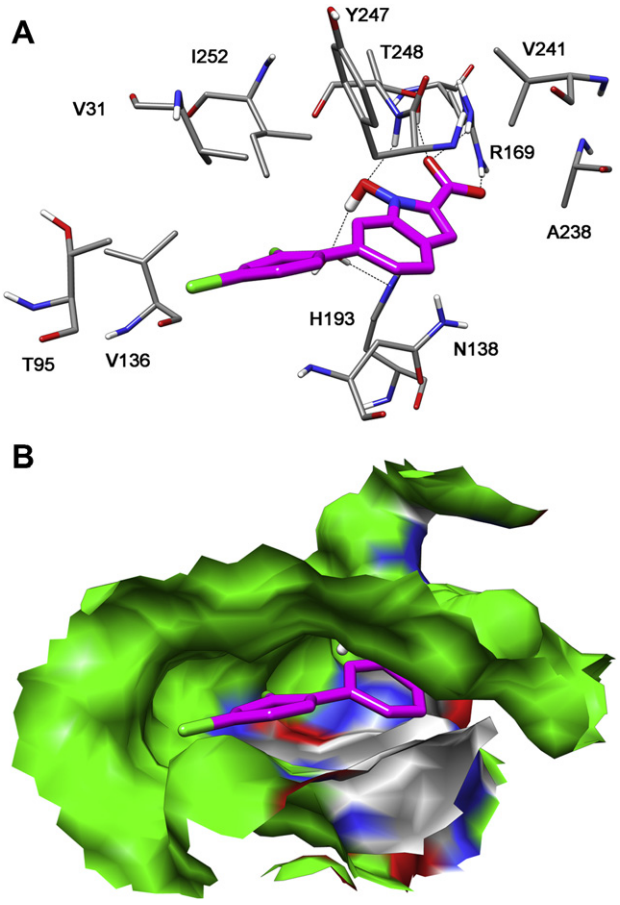

Fig. 4. MD simulation results for the complex of LDH-A with **3g**: main protein–ligand interactions (A) and surface analysis (B, hydrophobic regions are coloured green). (For interpretation of the references to colour in this figure legend, the reader is referred to the web version of this article.)

in a lipophilic cleft (see Fig. 4B) and shows interactions with V31, T95, V136 and Y247. The analysis of the volume of the cavities placed around **3g** in the enzyme active site reveals that there is a large empty space near the *p*-chloro-atom of the aryl substituent (region A of Fig. 5). Similarly, there is a certain space in correspondence of the 5 position of the indole ring (region B of Fig. 5) and this evidence is in accord with the fact that a few 5-aryl-substituted (**3a**,**e**) or 5,6-diphenyl-substituted (**3t**) NHI-derivatives give appreciable levels of LDH-inhibition. Nevertheless, these modelling results support the evidence that larger groups can be profitably tolerated in position 6, since this position points toward the enzyme entrance channel, and this is also consistent with the general higher activity associated to 6-aryl-substituted NHIs.

Overall, these results confirm that the NHI-based inhibitors herein reported may occupy both the substrate pocket, delimited by R169 and T248 and, in part, the cofactor pocket of the enzyme active site, placed around the enzyme entrance channel. This is in fine agreement with the experimental enzyme inhibition data, which indicate that they are competitive with both pyruvate and NADH.

5. Antiproliferative activities against cancer cells

The growth inhibitory effect of some selected NHI derivatives was assayed on two human pancreatic carcinoma cell lines, PANC-1 and MIA PaCa-2, whereas possible unspecific cytotoxicity was tested with a normal immortalized cell line of human foreskin fibroblast cells Hs27. During these experiments, cancer cells were exposed to both normoxic and hypoxic (1% of oxygen) conditions. Treatment of cells with LDH-inhibitors for 48 h resulted in a dose-dependent decline in cell viability and the effects of these

Table 2
Hydrogen bonds analysis of the enzyme-**3g** interactions during the last 7 ns of MD simulation.

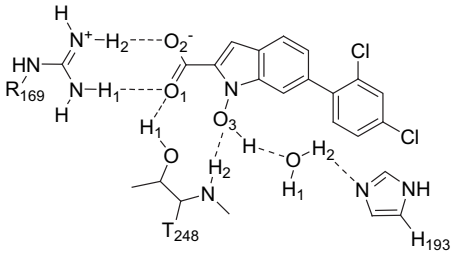

donor[a]	acceptor	acceptor	distance (Å)	% occupied
WAT@O	LIG@H	LIG@O3	2.7	99
H193@N	WAT@H1/2	WAT@O	2.8	84
LIG@O1	T248@H1	T248@OG1	2.7	79
LIG@O1	R169@H1	R169@NH1	2.8	76
LIG@O2	R169@H2	R169@NH2	2.8	71
LIG@O3	T248@H2	T248@N	2.9	49

[a] WAT = water, LIG = ligand **3g**.

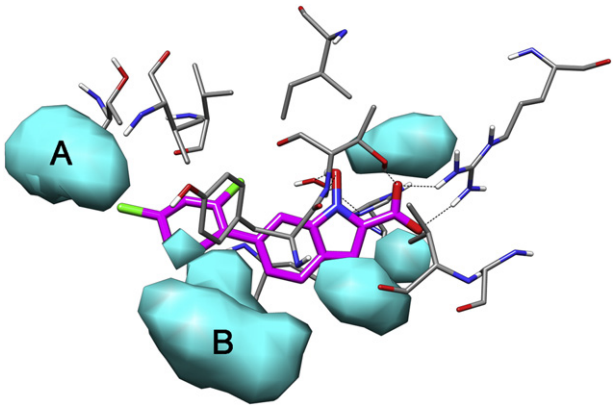

Fig. 5. Cavities (light blue) around **3g** and LDH active site. (For interpretation of the references to colour in this figure legend, the reader is referred to the web version of this article.)

Table 3
Antiproliferative activities (IC_{50}) of selected NHI derivatives on two pancreatic cancer cell lines.

Compound	PANC-1 (IC_{50}, μM)[a]		MIA PaCa-2 (IC_{50}, μM)[a]	
	normoxia[b]	hypoxia[c]	normoxia[b]	hypoxia[c]
3f	11.9	3.5	8.3	3.6
3g	12.0	2.0	6.8	1.8
3i	8.8	2.5	8.9	1.6
3o	10.2	2.3	5.8	2.2
3r	11.3	1.9	6.8	2.0
3t	11.3	2.3	7.8	1.9

[a] IC_{50}, Inhibitory concentration causing a 50% reduction in cell growth, in μM; mean values of at least 2 triplicate cytotoxicity sulphorhodamine-B (SRB) experiments are reported; the error in these values is within ±30% of the average.
[b] Normoxic conditions: 20–21% (v/v) O_2.
[c] Hypoxic conditions: 1% (v/v) O_2.

compounds on cell growth in both normoxic and hypoxic environments are reported in Table 3 as IC_{50} values.

All the tested LDH-inhibitors are active against these pancreatic cancer cells. Under normoxic conditions, the IC_{50} values against PANC-1 are in the 8.8–12.0 μM range, whereas MIA PaCa-2 cells are slightly more sensitive to these compounds, showing IC_{50} values which are always below 10 μM (5.8–8.9 μM). Most importantly, the anti-proliferative activity against both cancer cell lines turns out to be enhanced in hypoxia, with IC_{50}s generally dropping at around 2 μM for almost all the tested compounds. This phenomenon had already been observed with previously reported LDH inhibitors [22a], and is consistent with the fact that cancer cells rely more on LDH activity upon oxygen deprivation than under normally oxygenated conditions. This "addiction" to glycolysis may be exploited in a strategy recently defined as "synthetic lethal interactions" [32], where the two concurring factors leading to a cooperative cytotoxicity are hypoxia and blockade of glycolysis.

The selective cytotoxicity against cancer cells is supported by the fact that all these compounds showed IC_{50} values greater than 100 μM on Hs27 fibroblast cells, with the single exception constituted by **3i**, which displays a residual toxicity on these cells (IC_{50} = 68 μM).

6. Conclusions

Following our initial discovery of a new set of NHI-based *h*LDH5-inhibitors [22], in this study, we have further developed and optimized this class, by appropriately modifying the position and the type of the aryl-substituents present in the NHI scaffold. To the best of our knowledge, some of the compounds herein described represent the most potent and selective *h*LDH5-inhibitors ever reported in the literature. Their activity against invasive pancreatic cancer cell lines was confirmed under both normoxic and hypoxic conditions, although it is still too early to make any prediction about *in vivo* activities of these compounds. Overall, these findings contribute to shed light on the main pharmacophore characteristics needed for an efficient inhibition of this relatively new anti-cancer target. Moreover, they constitute important starting points for further molecular optimization in an attempt to develop new anti-tumour agents targeting the peculiar glucose metabolism of cancer cells.

7. Experimental section

7.1. Chemistry

7.1.1. General

Commercially available chemicals were purchased from Sigma–Aldrich or Alfa Aesar and used without further purification. NMR spectra were obtained with a Varian Gemini 200 MHz spectrometer. Chemical shifts (δ) are reported in parts per million (ppm) downfield from tetramethylsilane and referenced from solvent references (DMSO-d_6: δ_H = 2.50, δ_C = 39.52 ppm; acetone-d_6: δ_H = 2.05, δ_C = 29.84 ppm). Electron impact (EI, 70 eV) mass spectra were obtained on a Thermo Quest Finningan (TRACE GCQ plus) mass spectrometer. Purity was routinely measured by HPLC on a Waters SunFire RP 18 (3.0 × 150 mm, 5 μm) column (Waters, Milford, MA, www.waters.com) using a Beckmann SystemGold instrument consisting of chromatography 125 Solvent Module and a 166 UV Detector. Mobile phases: 10 mM ammonium acetate in Millipore purified water (A) and HPLC grade acetonitrile (B). A gradient was formed from 5% to 80% of B in 10 min and held at 80% for 10 min; flow rate was 0.7 mL/min and injection volume was 30 μL. HPLC purity of final compounds was determined by monitoring at 254 and 300 nm and was found to be ≥98%; retention times (HPLC, t_R) are given in minutes (min). Chromatographic separations were performed on silica gel columns by flash (Kieselgel 40, 0.040–0.063 mm; Merck) or gravity column (Kieselgel 60, 0.063–0.200 mm; Merck) chromatography. Reactions were followed by thin-layer chromatography (TLC) on Merck aluminum silica gel (60 F_{254}) sheets that were visualized under a UV lamp. Evaporation was performed in vacuo (rotating evaporator). Sodium sulphate was always used as the drying agent. Microwave assisted reaction were run in a CEM or Biotage microwave synthesizer. Characterization data of non-key compounds are reported in the Supplementary Data.

7.1.2. General procedure for the formation of nitrotoluene derivatives ***8a-e***

Method *A* A solution of $Pd(OAc)_2$ (25.2 mg, 0.112 mmol) and triphenylphosphine (147 mg, 0.560 mmol) in absolute ethanol (4 mL) and anhydrous toluene (4 mL) was stirred at RT under nitrogen for 10 min. After that period, commercially available 5-chloro-2-nitrotoluene **4** (646 mg, 3.76 mmol), 4 mL of 2M aqueous Na_2CO_3, and the appropriate boronic acid $R^1B(OH)_2$ (6.03 mmol) were sequentially added. The resulting mixture was heated at 100 °C in a sealed vial under nitrogen overnight. After being cooled to RT, the mixture was diluted with water and extracted with EtOAc. The combined organic phase were dried and concentrated. The crude product was purified by flash chromatography over silica gel column using *n*-Hex/EtOAc or $CHCl_3$/MeOH mixtures as the eluent. *Method B* Commercially available 5-chloro-2-nitrotoluene **4** (429 mg, 2.50 mmol) was placed in a vial together with the appropriate boronic acid $R^1B(OH)_2$ (2.50 mmol), sodium

carbonate (794 mg, 7.50 mmol), $Pd(OAc)_2$ (2.2 mg, 0.010 mmol), tetrabutylammonium bromide (805 mg, 2.50 mmol) and water (5 mL). The vial was sealed and heated under stirring at 175 °C in a microwave reactor for 5–10 min. The reaction mixture was then diluted with water and repeatedly extracted with EtOAc. The combined organic phase was dried over anhydrous sodium sulphate and evaporated to afford a crude residue that was purified by column chromatography over silica gel using *n*-Hex/EtOAc mixtures as the eluent.

*7.1.3. General procedure for the formation of nitrotoluene derivatives **8f–m, p**.*

Commercially available 4-bromo-2-nitrotoluene (**5**) and the appropriate boronic acid of general formula $R^2B(OH)_2$ were submitted to the same procedure described above for *"Method A"*, under either conventional heating at 100 °C, or microwave irradiation. In two cases (**8h,i**, Scheme 1), the use of potassium phosphate (3.93 mmol, for 2.31 mmol of **5**) as the base in water (0.5 mL) and conventional heating at 125 °C for 48 h in a sealed vial was preferred.

*7.1.4. General procedure for the formation of nitrotoluene derivatives **8n,o,q–s***

Commercially available aryl bromide of general formula R^2Br (1.76 mmol) was placed in a vial together with 4-methyl-3-nitrobenzeneboronic acid **6** (350 mg, 1.94 mmol), sodium carbonate (560 mg, 5.28 mmol), $Pd(OAc)_2$ (1.6 mg, 0.0070 mmol), tetrabutylammonium bromide (567 mg, 1.76 mmol) and water (5.5 mL). The vial was sealed and heated under stirring at 150 °C in a microwave reactor for 5–10 min. The reaction mixture was then diluted with water and repeatedly extracted with EtOAc. The combined organic phase was dried over anhydrous sodium sulphate and evaporated to afford a crude residue that was purified by column chromatography over silica gel using *n*-Hex/EtOAc mixtures as the eluent.

*7.1.5. Procedure for the formation of nitrotoluene derivative **8t***

1,2-Dichloro-4-methyl-5-nitrobenzene (**7**) [25] (460 mg, 2.23 mmol) was placed in a vial together with phenylboronic acid (1.09 g, 8.93 mmol), potassium phosphate (2.08 g, 9.81 mmol), $Pd(OAc)_2$ (13 mg, 0.059 mmol), tetrabutylammonium bromide (1.12 g, 34.6 mmol) and water (5 mL). The vial was sealed and heated under stirring at 125 °C for 48 h. The reaction mixture was cooled to RT and then diluted with water. The water phase was acidified with 1 N aqueous HCl and repeatedly extracted with EtOAc. The combined organic phase was dried over anhydrous sodium sulphate and evaporated to afford a crude residue that was purified by column chromatography over silica gel using *n*-hexane as the eluent, to give pure **8t** (587 mg, 2.03 mmol, 91% yield).

*7.1.6. General procedure for the formation of N-hydroxyindole methyl-esters **9***

Method C A stirred suspension of sodium hydride (60% dispersion in mineral oil, 263 mg, 6.58 mmol) in 4 mL of anhydrous DMF cooled to −15 °C under nitrogen was treated dropwise with a solution containing the appropriate nitrotoluene precursor **8** (1.64 mmol) and dimethyl oxalate (968 mg, 8.20 mmol) in 3 mL of anhydrous DMF. The mixture was left under stirring at the same temperature for 10 min and then it was slowly warmed to room temperature. Stirring at RT was continued until the disappearance of the precursor was verified by TLC. Then, the reaction mixture was slowly poured in an ice-water mixture; the water phase was acidified with 1 N aqueous HCl and extracted several times with EtOAc. The combined organic phase was washed with saturated $NaHCO_3$ solution and brine, then dried over anhydrous sodium sulphate. Evaporation under vacuum of the organic solvent afforded a crude product which was quickly filtered through a short column of silica gel using *n*-hexane/EtOAc mixtures as the eluent. The resulting α-ketoester intermediate was directly dissolved in anhydrous DME (2 mL) and the resultant solution was added dropwise to a cooled (0 °C) solution of $SnCl_2 \cdot 2H_2O$ (860 mg, 3.80 mmol) in DME (2 mL) containing 4Å molecular sieves, previously activated for 18 h at 130 °C in oven and cooled to RT in a desiccator over anhydrous calcium chloride. The reaction mixture was stirred under nitrogen at RT for 5 h, then it was monitored by TLC until disappearance of starting material (6–16 h). In some cases additional portions (1 eq. each) of $SnCl_2 \cdot 2H_2O$ were required to promote substrate conversion. The mixture was then diluted with water and repeatedly extracted with EtOAc. The combined organic phase was dried over anhydrous sodium sulphate and evaporated to afford a crude residue that was purified by column chromatography over silica gel using *n*-Hex/EtOAc or $CHCl_3$/MeOH mixtures as the eluent. *Method D*. The nitrotoluene precursor **8** (0.30 mmol) was submitted to the same initial treatment with sodium hydride and dimethyl oxalate as described above in "*Method C*". Then the resulting α-ketoester intermediate was transferred to a yellow suspension, previously generated by adding triethylamine (0.18 mL, 0.13 g, 1.3 mmol) dropwise to a stirred solution of $SnCl_2 \cdot 2H_2O$ (88.3 mg, 0.391 mmol) and thiophenol (0.12 mL, 0.13 g, 1.2 mmol) in acetonitrile (2.1 mL) at room temperature for 5 min. Upon consumption of starting material (typically within 5 min), the mixture was diluted with water and repeatedly extracted with EtOAc. The combined organic phase was dried over anhydrous sodium sulphate, diluted with toluene and treated with a catalytic amount of *p*-toluensulfonic acid. Then it was evaporated to promote the azeotropic dehydration of small amounts of hydrated precursors of NHIs **9**, affording a crude residue that was purified by column chromatography over silica gel using *n*-Hexane/EtOAc or $CHCl_3$/MeOH mixtures 7:3 as the eluent. *Method E*. The nitrotoluene precursor **8** (0.30 mmol) was submitted to the same initial treatment with sodium hydride and dimethyl oxalate as described above in "*Method C*". Then the resulting α-ketoester intermediate was dissolved in THF (0.5 mL) and the resulting solution was added to an aqueous solution (0.5 mL) of sodium hypophosphite monohydrate (88.4 g, 0.834 mmol). Then 2.7 mg of 10% palladium over charcoal was added and the resulting suspension was stirred at RT. Then it was monitored by TLC and additional portions of $H_2PO_2NaH_2O$ (88.4 g, 0.834 mmol) and Pd/C (2.7 mg) were added, if necessary. After disappearance of the precursor (TLC), typically after 24 h, the mixture was concentrated, diluted with water and repeatedly extracted with EtOAc. The combined organic phase was dried over anhydrous sodium sulphate and evaporated to afford a crude residue that was purified by column chromatography over silica gel using *n*-Hex/EtOAc or $CHCl_3$/MeOH mixtures as the eluent. *Method F*. The nitrotoluene precursor **8** (0.40 mmol) was submitted to the same initial treatment with sodium hydride and dimethyl oxalate as described above in "*Method C*". Then the α-ketoester intermediate (0.39 mmol) was dissolved in 4 mL of MeOH, and the resulting solution was treated with lead powder (400 mg, 1.93 mol) and 0.4 mL of triethylammonium formate. The mixture was stirred at 55 °C for 12 h, cooled to RT, and filtered over a pad of Celite. The solvent was removed under reduced pressure and the residue purified by column chromatography over silica gel using *n*-hexane/EtOAc 1:1 as the eluent.

*7.1.7. General procedure for the formation of N-hydroxyindole-2-carboxylates **3***

Methyl esters **9** (0.16 mmol) were dissolved in a 1:1 mixture of THF/methanol (3 mL) and treated with 0.5 mL of 2 N aqueous solution of LiOH. The reaction was kept under stirring in the dark at

RT and it was monitored by TLC. Upon consumption of starting material, the reaction mixture was concentrated, diluted with water and washed with Et_2O. The aqueous phase was treated with 1 N aqueous HCl and extracted several times with EtOAc. The combined ethyl acetate organic phase was dried over anhydrous sodium sulphate and evaporated to afford the desired *N*-hydroxyindol-carboxylic acid products **3**.

*7.1.7.1. 5-(4-Chlorophenyl)-1-hydroxy-1H-indole-2-carboxylic acid (**3a**).* Yield 99%; ^{1}H NMR (200 MHz, DMSO-d_6) δ (ppm): 7.07 (s, 1H), 7.44–7.56 (m, 3H), 7.63 (dd, 1H, J = 8.7, 1.6 Hz), 7.71 (AA′/XX′, 2H, J_{Ax} = 8.6 Hz, $J_{AA'/xx'}$ = 1.5 Hz), 7.93 (d, 1H, J = 0.8 Hz); ^{13}C NMR (50 MHz, DMSO-d_6) δ (ppm): 105.11, 110.24, 120.07, 121.44, 124.08, 127.43, 128.38 (2C), 128.78 (2C), 131.42, 135.46, 139.70, 161.10; MS (EI, 70 eV) *m/z* (%): 289 (40) [^{37}Cl, M$^+$], 287 (100) [^{35}Cl, M$^+$], 271 (85) [^{37}Cl, M$^+$ −H_2O, ^{35}Cl, M$^+$ −O]; HPLC, t_R = 9.9 min.

*7.1.7.2. 5-(3-Carboxyphenyl)-1-hydroxy-1H-indole-2-carboxylic acid (**3e**).* Yield 84%; ^{1}H NMR (200 MHz, acetone-*d6*) δ (ppm): 7.18 (d, 1H, J = 0.9 Hz), 7.58 (td, 1H, J = 7.5, 0.4 Hz), 7.62 (dt, 1H, J = 8.8, 0.7 Hz), 7.71 (dd, 1H, J = 8.6, 1.6 Hz), 7.91 (dd, 1H, J = 2.0, 1.3 Hz), 7.94–8.00 (m, 2H), 8.31 (t, 1H, J = 1.6 Hz); ^{13}C NMR (50 MHz, acetone-*d6*) δ (ppm): 106.66, 111.07, 121.52, 123.01, 125.70, 128.60, 128.80, 129.89, 132.10, 132.21, 133.81, 136.50, 139.10, 142.78, 162.00, 167.49; MS (EI, 70 eV) *m/z* (%): 297 (10) [M$^+$], 281 (60) [M$^+$ −O], 248 (100) [M$^+$ −O_2 −OH]; HPLC, t_R = 5.8 min.

*7.1.7.3. 6-(4-Chlorophenyl)-1-hydroxy-1H-indole-2-carboxylic acid (**3f**).* Yield 93%; ^{1}H NMR (200 MHz, DMSO-*d6*) δ (ppm): 7.04 (d, 1H, J = 0.8 Hz), 7.41 (dd, 1H, J = 8.4, 1.4 Hz), 7.52 (AA'XX', 2H, *JAX* = 8.4 Hz, *JAA'/XX'* = 2.0 Hz), 7.65 (s, 1H), 7.68–7.82 (m, 3H); ^{13}C NMR (50 MHz, DMSO-*d6*) δ (ppm): 104.49, 107.16, 119.71, 120.58, 122.77, 127.52, 128.58 (2C), 128.85 (2C), 132.04, 135.53, 136.31, 139.39, 161.08; MS (EI, 70 eV) *m/z* (%): 289 (15) [^{37}Cl, M$^+$], 287 (36) [^{35}Cl, M$^+$] 273 (22) [^{37}Cl, M$^+$ −O], 271 (56) [^{35}Cl, M$^+$ −O], 190 (100) [M$^+$ −Cl −H_2O −CO_2]; HPLC, t_R = 10.2 min.

*7.1.7.4. 6-(2,4-Dichlorophenyl)-1-hydroxy-1H-indole-2-carboxylic acid (**3g**).* Yield 99%; ^{1}H NMR (200 MHz, acetone-*d6*) δ (ppm): 7.17 (d, 1H, J = 0.9 Hz), 7.20 (dd, 1H, J = 8.4, 1.6 Hz), 7.48 (dd, 1H, J = 8.3, 1.7 Hz), 7.53 (dd, 1H, J = 8.4, 0.7 Hz), 7.58 (dt, 1H, J = 1.5, 0.7 Hz), 7.64 (dd, 1H, J = 1.7, 0.6 Hz), 7.76 (dd, 1H, J = 8.4, 0.7 Hz); ^{13}C NMR (50 MHz, acetone-*d6*) δ (ppm): 106.06, 111.12, 122.05, 122.98, 123.25, 127.45, 128.24, 130.20, 133.72, 133.90, 134.14, 136.10, 136.61, 140.58, 161.98; MS (EI, 70 eV) *m/z* (%): 325 (5) [$^{37/37}$Cl2, M$^+$], 323 (23) [$^{37/35}$Cl2, M$^+$], 321 (36) [$^{35/35}$Cl2, M$^+$], 309 (6) [$^{37/37}$Cl2, M$^+$ −O], 307 (29) [$^{37/35}$Cl2, M$^+$ −O], 305 (44) [$^{35/35}$Cl2, M$^+$ −O], 226 (37) [^{37}Cl, M$^+$ −Cl −OH −COOH]; 224 (100) [^{35}Cl, M$^+$ −Cl −OH −COOH]; 189 (74) [M$^+$ −2Cl −OH −COOH]; HPLC, t_R = 11.3 min.

*7.1.7.5. 6-(4-Fluorophenyl)-1-hydroxy-1H-indole-2-carboxylic acid (**3h**).* Yield 93%; ^{1}H NMR (200 MHz, acetone-*d6*) δ (ppm): 7.15 (d, 1H, J = 0.6 Hz), 7.18–7.32 (m, 2H), 7.42 (dd, 1H, J = 8.6, 1.6 Hz), 7.67–7.86 (m, 4H); ^{13}C NMR (50 MHz, acetone-*d6*) δ (ppm): 106.19, 108.17, 116.32 (d, 2C, J = 21.0 Hz), 121.26, 121.77, 123.68, 127.13, 129.79 (d, 2C, J = 8.2 Hz), 137.50, 138.14, 138.52 (d, J = 3.7 Hz), 161.90, 163.15 (d, J = 244.5 Hz); MS (EI, 70 eV) *m/z* (%): 271 (100) [M$^+$], 255 (33) [M$^+$ −O], 208 (55) [M$^+$ −CO2 −F]; HPLC, t_R = 9.7 min.

*7.1.7.6. 1-Hydroxy-6-(4-(trifluoromethyl)phenyl)-1H-indole-2-carboxylic acid (**3i**).* Yield 89%; ^{1}H NMR (200 MHz, acetone-*d6*) δ (ppm): 7.17 (d, 1H, J = 0.7 Hz), 7.52 (dd, 1H, J = 8.4, 1.6 Hz), 7.81 (dd, 1H, J = 8.4, 0.7 Hz), 7.82–7.90 (m, 3H), 7.96–8.03 (m, 2H); ^{13}C NMR (50 MHz, acetone-*d6*) δ (ppm): 106.00, 108.83, 121.23, 122.45, 123.94, 125.48 (q, J = 269.7 Hz), 126.54 (q, 2C, J = 3.7 Hz), 127.60, 128.62 (2C), 129.35 (q, J = 34.8 Hz), 137.36, 137.38, 146.10, 161.99; MS (EI, 70 eV) *m/z* (%): 321 (100) [M$^+$], 305 (18) [M$^+$ −O]; HPLC, t_R = 10.4 min.

*7.1.7.7. 6-(Biphenyl-4-yl)-1-hydroxy-1H-indole-2-carboxylic acid (**3j**).* Yield 93%; ^{1}H NMR (200 MHz, acetone-*d6*) δ (ppm): 7.16 (d, 1H, J = 0.7 Hz), 7.34–7.56 (m, 3H), 7.72–7.90 (m, 9H); ^{13}C NMR (50 MHz, acetone-*d6*) δ (ppm): 106.10, 108.23, 121.37, 122.12, 123.78, 126.29, 127.65 (2C), 128.18, 128.26 (2C), 128.51 (2C), 129.77 (2C), 137.54, 138.85, 140.84, 141.33, 141.44, 162.40; MS (EI, 70 eV) *m/z* (%): 329 (10) [M$^+$], 313 (100) [M$^+$ −O], 267 (41) [M$^+$ −OH −COOH], 190 (27) [M$^+$ −OH −COOH −C6H5]; HPLC, t_R = 10.4 min.

*7.1.7.8. 1-Hydroxy-6-(naphthalen-1-yl)-1H-indole-2-carboxylic acid (**3k**).* Yield 82%; ^{1}H NMR (200 MHz, DMSO-*d6*) δ (ppm): 7.11 (d, 1H, J = 0.9 Hz), 7.21 (dd, 1H, J = 8.2, 1.6 Hz), 7.45–7.64 (m, 5H), 7.77 (dd, 1H, J = 8.2, 0.6 Hz), 7.86 (dd, 1H, J = 7.9, 1.3 Hz), 7.97 (d, 1H, J = 8.6 Hz), 8.02 (dd, 1H, J = 7.9, 1.6 Hz); ^{13}C NMR (50 MHz, DMSO-*d6*) δ (ppm): 104.65, 110.28, 120.26, 121.97, 122.84, 125.30, 125.50, 125.83, 126.24, 126.99, 127.34, 127.48, 128.28, 130.94, 133.38, 135.99, 136.66, 139.86, 161.06; MS (EI, 70 eV) *m/z* (%): 303 (53) [M$^+$], 287 (87) [M$^+$ −O], 241 (100) [M$^+$ −OH −COOH]; HPLC, t_R = 10.3 min.

*7.1.7.9. 1-Hydroxy-6-(naphthalen-2-yl)-1H-indole-2-carboxylic acid (**3l**).* Yield 99%; ^{1}H NMR (200 MHz, acetone-*d6*) δ (ppm): 7.17 (d, 1H, J = 0.9 Hz), 7.51–7.57 (m, 2H), 7.63 (dd, 1H, J = 8.5, 1.6 Hz), 7.81 (dd, 1H, J = 8.4, 0.6 Hz), 7.92–7.97 (m, 3H), 7.99–8.06 (m, 2H), 8.29 (d, 1H, J = 1.5 Hz); ^{13}C NMR (50 MHz, DMSO-*d6*) δ (ppm): 104.52, 107.40, 120.09, 120.40, 120.49, 122.68, 125.23 (2C), 125.95, 126.30, 127.37, 128.14, 128.39, 132.09, 133.35, 136.50, 136.68, 137.86, 161.08; MS (EI, 70 eV) *m/z* (%): 303 (44) [M$^+$], 287 (100) [M$^+$ −O], 241 (57) [M$^+$ −OH −COOH]; HPLC, t_R = 10.1 min.

*7.1.7.10. 1-Hydroxy-6-(4-(trifluoromethoxy)phenyl)-1H-indole-2-carboxylic acid (**3n**).* Yield 55%; ^{1}H NMR (200 MHz, acetone-*d6*) δ (ppm): 7.16 (d, 1H, J = 0.9 Hz), 7.42–7.50 (m, 3H), 7.75–7.80 (m, 2H), 7.88 (AA′XX′, 2H, JAX = 8.9 Hz, JAA′/XX′ = 2.6 Hz); ^{13}C NMR (50 MHz, acetone-*d6*) δ (ppm): 106.02, 108.48, 121.23, 121.43 (q, J = 256.5 Hz), 122.06, 122.23 (2C), 123.81, 127.34, 129.66 (2C), 137.36, 137.60, 141.42, 149.21, 161.98; MS (EI, 70 eV) *m/z* (%): 337 (100) [M$^+$], 321 (74) [M$^+$ −O], 293 (7) [M$^+$ −CO_2], 275 (22) [M$^+$ −CO_2 −H_2O], 249 (26) [M$^+$ −CO_2 −H_2O −C_2H_2]; HPLC, t_R = 10.3 min.

*7.1.7.11. 1-Hydroxy-6-(3-(trifluoromethoxy)phenyl)-1H-indole-2-carboxylic acid (**3o**).* Yield 83%; ^{1}H NMR (200 MHz, acetone-*d6*) δ (ppm): 7.16 (d, 1H, J = 0.7 Hz), 7.31–7.38 (m, 1H), 7.49 (dd, 1H, J = 8.4, 1.6 Hz), 7.63 (t, 1H, J = 7.9 Hz), 7.68–7.70 (m, 1H), 7.77–7.83 (m, 3H); ^{13}C NMR (50 MHz, acetone-*d6*) δ (ppm): 105.95, 108.72, 120.34, 120.55, 121.23, 121.62 (q, J = 253.4 Hz), 122.41, 123.94, 126.94, 127.53, 131.48, 137.31, 137.49, 144.81, 150.62, 162.27; MS (EI, 70 eV) *m/z* (%): 337 (76) [M$^+$], 321 (100) [M$^+$ −O], 293 (8) [M$^+$ −CO_2], 275 (13) [M$^+$ −CO_2 −H_2O], 249 (21) [M$^+$ −CO_2 −H_2O −C_2H_2]; HPLC, t_R = 10.4 min.

*7.1.7.12. 6-(Furan-3-yl)-1-hydroxy-1H-indole-2-carboxylic acid (**3s**).* Yield 97%; ^{1}H NMR (200 MHz, acetone-d_6) δ (ppm): 7.01 (dd, 1H, J = 1.8, 0.9 Hz), 7.10 (d, 1H, J = 0.9 Hz), 7.42 (dd, 1H, J = 8.4, 1.5 Hz), 7.65–7.72 (m, 3H), 8.13 (dd, 1H, J = 1.5, 0.9 Hz); ^{13}C NMR (50 MHz, acetone-d_6) δ (ppm): 106.24, 106.75, 109.61, 120.33, 121.52, 123.59, 127.75, 129.64, 130.64, 137.34, 140.02, 144.86, 162.14; MS (EI, 70 eV) *m/z* (%): 243 (56) [M$^+$], 227 (100) [M$^+$ −O], 180 (26) [M$^+$ −CO_2 −H_2O]; HPLC, t_R = 8.6 min.

*7.1.7.13. 1-Hydroxy-5,6-diphenyl-1H-indole-2-carboxylic acid (**3t**).* Yield 80%; ^{1}H NMR (200 MHz, acetone-d_6) δ (ppm): 7.06–7.28 (m, 11H), 7.54 (s, 1H), 7.70 (s, 1H); ^{13}C NMR (50 MHz, acetone-d_6) δ (ppm): 106.28, 111.80, 121.88, 124.85, 126.80, 127.18, 127.51, 128.49 (2C), 128.56 (2C), 130.73 (2C), 130.84 (2C), 135.32, 136.47, 139.65, 142.93, 143.02, 162.01; MS (EI, 70 eV) *m/z* (%): 330 (15) [M + H$^+$], 268 (100) [M$^+$ −CO_2 −H_2O], 254 (31) [M$^+$ −CO_2 −NOH]; HPLC, t_R = 10.3 min.

7.2. Molecular modelling

Compound **3g** was built using Maestro 9.0 [33] and was minimized using the conjugate gradient method until a convergence value of 0.05 kcal/(mol•Å) was reached. The minimization was carried out in a water environment model (generalized-Born/surface-area model) using the MMFFs force field and a distance-dependent dielectric constant of 1.0. The human muscle L-LDH M chain was extracted from the minimized average structure of the LDH obtained by us through molecular dynamic simulations [22]. Automated docking was carried out by means of the GOLD program, version 4.1.1 [34]. The "allow early termination" option was deactivated, the remaining GOLD default parameters were used, and the ligand was submitted to 30 genetic algorithm runs by applying the ChemScore fitness function. The best docked conformation was taken into account. The so obtained complex was energy minimized using AMBER 11 [35]. The complex was placed in a rectangular parallelepiped water box, an explicit solvent model for water (TIP3P) was used, and the complex was solvated with a 10 Å water cap. Chlorine ions were added as counterions to neutralize the system. Two steps of minimization were then carried out. In the first stage, we kept the complex fixed with a position restraint of 500 kcal/(mol•Å^2) and we solely minimized the positions of the water molecules. In the second stage, we minimized the entire system through 20 000 steps of steepest descent followed by conjugate gradient until a convergence of 0.05 kcal/(mol•Å) was attained. All the α carbons of the protein were blocked with a harmonic force constant of 10 kcal/(mol•Å^2). Ten nanoseconds of MD simulation were then carried out. The time step of the simulations was 2.0 fs with a cutoff of 10 Å for the non-bonded interaction, and SHAKE was employed to keep all bonds involving hydrogen atoms rigid. Constant-volume periodic boundary MD was carried out for 400 ps, during which the temperature was raised from 0 to 300 K. Then 9.6 ns of constant pressure periodic boundary MD was carried out at 300 K using the Langevin thermostat to maintain constant the temperature of our system. In the first 1.2 ns, all the α carbons of the protein were blocked with a harmonic force constant, which decreased during these 1.2 ns from 10 to 1 kcal/(mol•Å^2), while in the last 7.8 ns, no constraints were applied. General Amber force field (GAFF) parameters were assigned to the ligand, while partial charges were calculated using the AM1-BCC method as implemented in the Antechamber suite of AMBER 11. The final structure of the complex was obtained as the average of the last 7 ns of MD minimized by the CG method until a convergence of 0.05 kcal/(mol•Å). The average structure was obtained using the ptraj program implemented in AMBER 11.

7.3. Biological methods

7.3.1. Enzyme kinetics experiments

The LDH inhibitory activities of the new compounds were measured by standard enzyme kinetics experiments, by means of spectrophotometric measurement (Lambda 25, PerkinElmer) of the oxidation of NADH at 340 nm (ε = 6.2 mM^{-1} cm^{-1}), which is a direct measure of the reduction of pyruvate to lactate. The effect of the perspective inhibitors on *h*LDH5 and *h*LDH1 enzyme activities were measured using commercially available purified human lactate dehydrogenase isoform 5 (*h*LDH5, LDH-A_4, LDH-A Lee Biosolution, Inc.) and isoform 1 (*h*LDH1, LDH-B_4, LDH-B, ERM® - AD453/IFCC from Sigma). The reaction velocity of purified human *h*LDH5 and *h*LDH1, and the values of optical density were determined at 30-s intervals for 5 min, by measuring the decrease in absorbance at 340 nm of NADH at 37 °C. The apparent Michaelis–Menten constants (K_m) of *h*LDH5 and *h*LDH1 were measured by non-linear regression analysis with the GraphPad Prism 3.0 from Lineweaver–Burk plots. The K_m values of *h*LDH5 for NADH and pyruvate were determined in saturating conditions as described below. In 100 mM sodium phosphate buffer (pH 7.4), 0.005 units of *h*LDH5 were combined with 2 mM sodium pyruvate (pyruvate-saturated) and 12.5 μM–150 μM NADH, or 200 μM NADH (NADH-saturated) and 25 μM to 1 mM sodium pyruvate, and these conditions were used for all assays. Under these conditions NADH showed a K_m of 20.0 μM and a V_{max} of 62.5 μmol/min/mg, whereas pyruvate showed a K_m of 120 μM and a V_{max} of 62.5 μmol/min/mg. Michaelis–Menten constants for substrates were determined from initial rate measurements at 37 °C by non-linear regression analysis with the GraphPad Prism 3.0. Briefly, the synthesized compounds were dissolved in stock solutions of DMSO (concentrations of DMSO during the initial rate measurements did not exceed 0.5%). Using 25 μM NADH and 2 mM sodium pyruvate we initially evaluated the percentual inhibition of the compounds. Then, we evaluated the apparent K_m' values in the presence of these inhibitors (concentration range = 5–100 μM). From the values of K_m' so obtained, K_i values for each single inhibitor were determined using double-reciprocal plots. The effect of the same compounds on *h*LDH1 enzyme activity was measured as described before for *h*LDH5, only in pyruvate-saturating conditions. Under these conditions NADH showed a K_m of 27 μM and a V_{max} of 65 μmol/min/mg. The inhibition percentage of these compounds at a fixed concentration of 125 μM was determined as described above.

7.3.2. Cell culture and cytotoxicity in normoxic and hypoxic exposure

Human pancreatic tumour cells PANC-1 (CRL-1469) and MIA PaCa-2 (CRL-1420), as well as skin fibroblasts Hs27 (CRL-1634), were obtained from the American Type Culture Collection (ATCC, Manassas, VA, USA). Cells were maintained in RPMI 1640 medium, supplemented with fetal calf serum (10%), glutamine (2 mM), and 1% penicillin-streptomycin (100 00U/ml), at 37 °C under an atmosphere of 5% CO_2. The cells were maintained in 75 cm^2 culture flasks (Greiner-Bio-One, Frickenhausen, Germany) and harvested with trypsin-EDTA (Invitrogen, Paisley, UK) at their exponential phase of growth phase. Chemosensitivity tests were performed using the SRB assay as described in the NCI protocol, with slight modifications. Selected compounds **3f,g,i,o,r,t** were dissolved in sterile DMSO at 2.5 mM and stored at −20 °C, in the dark. They were diluted in sterile culture medium immediately before their use. Cells were plated at $5 \cdot 10^4$ cells/well and each compound was tested in triplicate at different concentrations (1–100 μM), using the SRB assay as described previously [22]. Briefly, control cells were exposed to an equivalent concentration of DMSO (0.25% v/v, negative control). At the end of drug incubation (48 h), growth inhibition was expressed as the percentage of control absorbance (corrected for absorbance before drug addition). The 50% inhibitory concentration of cell growth (IC_{50}) was calculated by non-linear least squares curve fitting (GraphPad PRISM, Intuitive Software for Science, San Diego, CA). These experiments were also performed in cells under hypoxia conditions, using the incubator IncuSafe, (Labo Equipment Sanyo, UK). Hypoxic cells were maintained in a controlled atmosphere chamber with a gas mixture containing 1% (v/v) O_2, 5% (v/v) CO_2, and 94% (v/v) N_2 at 37 °C.

Acknowledgment

The research leading to these results has received funding (to FM and SR) from the European Union's Seventh Framework Programme (FP7-PEOPLE–IIF–2008) under grant agreement n. 235016 ("NOXYCANCERSTARV"). CG thanks the Italian Ministry for University and Research (MIUR) for a PhD fellowship. Siena Biotech S. p. A. - Italy, is gratefully acknowledged for a research contribution (FM). This work was also supported by a grant from the EORTC-PAMM group to FM and GJP. We thank Dr. Giorgio Placanica and Dr. Caterina Orlando for technical assistance in the analysis of the chemical products.

Appendix. Supplementary data

Supplementary data associated with this article can be found, in the online version, at doi:10.1016/j.ejmech.2011.08.046.

References

[1] D. Hanahan, R.A. Weinberg, Cell 144 (2011) 646–674.
[2] O. Warburg, Science 123 (1956) 309–314.
[3] (a) M.G. Vander Heiden, L.C. Cantley, C.B. Thompson, Science 324 (2009) 1029–1033;
(b) R.A. Gatenby, R.J. Gillies, Nat. Rev. Cancer 4 (2004) 891–899;
(c) R.A. Cairns, I.S. Harris, T.W. Mak, Nat. Rev. Canc. 11 (2011) 85–95.
[4] S. Ben-Haim, P. Ell, J. Nucl. Med. 50 (2009) 88–99.
[5] (a) C.V. Dang, M. Hamaker, P. Sun, A. Le, P. Gao, J. Mol. Med. 89 (2011) 205–212;
(b) G. Kroemer, J. Pouyssegur, Cancer Cell 13 (2008) 472–482;
(c) D.A. Tennant, R.V. Durán, E. Gottlieb, Nat. Rev. Canc. 10 (2010) 267–277;
(d) R. Scatena, P. Bottoni, A. Pontoglio, L. Mastrototaro, B. Giardina, Exp. Opin. Invest. Drugs 17 (2008) 1533–1534;
(e) S.P. Mathupala, Recent Pat. Anti-Canc. Drug Discov. 6 (2011) 6–14.
[6] (a) H.R. Christofk, M.G. Vander Heiden, M.H. Harris, A. Ramanathan, R.E. Gerszten, R. Wei, M.D. Fleming, S.L. Schreiber, L.C. Cantley, Nature 452 (2008) 230–233;
(b) M.G. Vander Heiden, H.R. Christofk, E. Schuman, A.O. Subtelny, H. Sharfi, E.E. Harlow, J. Xian, L.C. Cantley, Biochem. Pharmacol. 79 (2010) 1118–1124.
[7] (a) J.-K. Jiang, M.B. Boxer, M.G. Vander Heiden, M. Shen, A.P. Skoumbourdis, N. Southall, H. Veith, W. Leister, C.P. Austin, H.W. Park, J. Inglese, L.C. Cantley, D.S. Auld, C.J. Thomas, Bioorg. Med. Chem. Lett. 20 (2010) 3387–3393;
(b) M.B. Boxer, J.-K. Jiang, M.G. Vander Heiden, M. Shen, A.P. Skoumbourdis, N. Southall, H. Veith, W. Leister, C.P. Austin, H.W. Park, J. Inglese, L.C. Cantley, D.S. Auld, C.J. Thomas, J. Med. Chem. 53 (2010) 1048–1055.
[8] S. Bonnet, S.L. Archer, J. Allalunis-Turner, A. Haromy, C. Beaulieu, R. Thompson, C.T. Lee, G.D. Lopaschuk, L. Puttagunta, S. Bonnet, G. Harry, K. Hashimoto, C.J. Porter, M.A. Andrade, B. Thebaud, E.D. Michelakis, Cancer Cell 11 (2007) 37–51.
[9] K.E. Yen, M.A. Bittinger, S.M. Su, V.R. Fantin, Oncogene 29 (2010) 6409–6417.
[10] E. Goldberg, Exp. Clin. Immunogenet. 2 (1985) 120–124.
[11] J.A. Read, V.J. Winter, C.M. Eszes, R.B. Sessions, R.L. Brady, Proteins 43 (2001) 175–185.
[12] G.A. Brooks, H. Dubouchaud, M. Brown, J.P. Sicurello, C.E. Butz, Proc. Natl. Acad. Sci. USA 96 (1999) 1129–1134.
[13] (a) M.I. Koukorakis, A. Giatromanolaki, C. Simopoulos, A. Polychronidis, E. Sivridis, Clin. Experim. Metast 22 (2005) 25–30;
(b) M.I. Koukorakis, M. Pitiakoudis, A. Giatromanolaki, A. Tsarouha, A. Polychronidis, E. Sivridis, C. Simopoulos, Cancer Sci. 97 (2006) 1056–1060;
(c) M.I. Koukourakis, A. Giatromanolaki, E. Sivridis, K.C. Gatter, T. Trarbach, G. Folprecht, M.M. Shi, D. Lebwohl, T. Jalava, D. Laurent, G. Meinhardt, A.L. Harris, Clin. Cancer Res. 17 (2011) 4892–4900.
[14] (a) B.S. Sørensen, J. Hao, J. Overgaard, H. Vorum, B. Honoré, J. Alsner, M.R. Horsman, Radiother. Oncol. 76 (2005) 187–193;
(b) B.S. Sørensen, J. Alsner, J. Overgaard, M.R. Horsman, Radiother. Oncol. 83 (2007) 362–366.
[15] (a) V.R. Fantin, J. St-Pierre, P. Leder, Cancer Cell. 9 (2006) 425–434;
(b) Z. -Y. Wang, T. Y. Loo, J. -G. Shen, N. Wang, D. -M. Wang, D. -P. Yang, S. -L. Mo, X. -Y. Guan, J. -P. Chen, Breast Cancer Res. Treat. 2011, in press.
[16] T. Kanno, K. Sudo, M. Maekawa, Y. Nishimura, M. Ukita, K. Fukutake, Clin. Chim. Acta 173 (1988) 89–98.
[17] C. Granchi, S. Bertini, M. Macchia, F. Minutolo, Curr. Med. Chem. 17 (2010) 672–697.
[18] L. Fiume, M. Manerba, M. Vettraino, G. Di Stefano, Pharmacology 86 (2010) 157–162.
[19] L.M. Deck, R.E. Royer, B.B. Chamblee, V.M. Hernandez, R.R. Malone, J.E. Torres, L.A. Hunsaker, R.C. Piper, M.T. Makler, D.L. Vander Jagt, J. Med. Chem. 41 (1998) 3879–3887.
[20] A. Le, C.R. Cooper, A.M. Gouw, R. Dinavahi, A. Maitra, L.M. Deck, R.E. Royer, D.L. Vander Jagt, G.L. Semenza, C.V. Dang, Proc. Natl. Acad. Sci. USA 107 (2010) 2037–2042.
[21] A.D. Moorhouse, C. Spiteri, P. Sharma, M. Zloh, J.E. Moses, Chem. Commun. 47 (2011) 230–232.
[22] (a) C. Granchi, S. Roy, C. Giacomelli, M. Macchia, T. Tuccinardi, A. Martinelli, M. Lanza, L. Betti, G. Giannaccini, A. Lucacchini, N. Funel, L.G. León, E. Giovannetti, G.J. Peters, R. Palchaudhuri, E.C. Calvaresi, P.J. Hergenrother, F. Minutolo, J. Med. Chem. 54 (2011) 1599–1612;
(b) C. Granchi, S. Roy, C. Del Fiandra, T. Tuccinardi, M. Lanza, L. Betti, G. Giannaccini, A. Lucacchini, A. Martinelli, M. Macchia, F. Minutolo, Med. Chem. Commun. 2 (2011) 638–643.
[23] N. Miyaura, A. Suzuki, Chem. Rev. 95 (1995) 2457–2483.
[24] N.E. Leadbeater, M. Marco, Org. Lett. 4 (2002) 2973–2976.
[25] R.B. Bedford, M.E. Blake, C.P. Butts, D. Holder, Chem. Commun. (2003) 466–467.
[26] I. Shimada, K. Maeno, K. Kazuta, H. Kubota, T. Kimizuka, Y. Kimura, K. Hatanaka, Y. Naitou, F. Wanibuchi, S. Sakamoto, S. Tsukamoto, Bioorg. Med. Chem. 16 (2008) 1966–1982.
[27] K.C. Nicolaou, A.A. Estrada, G.C. Freestone, S.H. Lee, X. Alvarez-Mico, Tetrahedron 63 (2007) 6088–6114.
[28] W. Dong, L.S. Jimenez, J. Org. Chem. 64 (1999) 2520–2523.
[29] (a) M. Bartra, P. Romea, F. Urpí, J. Vilarrasa, Tetrahedron 46 (1990) 587–594;
(b) D. Sawant, R. Kumar, P.R. Maulik, B. Kundu, Org. Lett. 8 (2006) 1525–1528.
[30] I.D. Entwistle, T. Gilkerson, R.A.W. Johnstone, R.P. Telford, Tetrahedron 34 (1978) 213–215.
[31] A. Wong, J.T. Kuethe, I.W. Davies, J. Org. Chem. 68 (2003) 9865–9866.
[32] D.A. Chan, A.J. Giaccia, Nat. Rev. Drug Discov. 10 (2011) 351–364.
[33] Maestro, Version 9.0. Schrödinger Inc, Portland, OR, 2009.
[34] M.L. Verdonk, J.C. Cole, M.J. Hartshorn, C.W. Murray, R.D. Taylor, Proteins 52 (2003) 609–623.
[35] D.A. Case, T.A. Darden, T.E. Cheatham III, C.L. Simmerling, J. Wang, R.E. Duke, R. Luo, R.C. Walker, W. Zhang, K.M. Merz, B. Roberts, B. Wang, S. Hayik, A. Roitberg, G. Seabra, I. Kolossvai, K.F. Wong, F. Paesani, J. Vanicek, J. Liu, X. Wu, S.R. Brozell, T. Steinbrecher, H. Gohlke, Q. Cai, X. Ye, J. Wang, M.-J. Hsieh, G. Cui, D.R. Roe, D.H. Mathews, M.G. Seetin, C. Sagui, V. Babin, T. Luchko, S. Gusarov, A. Kovalenko, P.A. Kollman, AMBER 11. University of California, San Francisco, 2010.